

Damage detection technique in existing structures using vibration-based model updating

Devesh K. Jaiswal^a, Goutam Mondal^{*}, Suresh R. Dash^b and Mayank Mishra^c

School of Infrastructure, Indian Institute of Technology Bhubaneswar, Bhubaneswar-752050, India

(Received September 10, 2021, Revised December 22, 2022, Accepted March 17, 2023)

Abstract. Structural health monitoring and damage detection are essential for assessing, maintaining, and rehabilitating structures. Most of the existing damage detection approaches compare the current state structural response with the undamaged vibrational structural response, which is unsuitable for old and existing structures where undamaged vibrational responses are absent. One of the approaches for existing structures, numerical model updating/inverse modelling, available in the literature, is limited to numerical studies with high-end software. In this study, an attempt is made to study the effectiveness of the model updating technique, simplify modelling complexity, and economize its usability. The optimization-based detection problem is addressed by using programmable open-sourced code, OpenSees[®] and a derivative-free optimization code, NOMAD[®]. Modal analysis is used for damage identification of beam-like structures with several damage scenarios. The performance of the proposed methodology is validated both numerically and experimentally. The proposed method performs satisfactorily in identifying both locations and intensity of damage in structures.

Keywords: damage detection; optimization; model updating; structural health monitoring; vibrational analysis

1. Introduction

Civil engineering structures undergo damage and deterioration during their life span, thereby reducing their service life. Since the high cost and time is involved in building these structures, it is necessary to monitor and maintain their integrity by employing efficient structural health monitoring (SHM) techniques (Inman *et al.* 2005, Moaveni *et al.* 2013, Nagarajaiah and Erazo 2016). A few past case studies indicate that the old existing structures have led to catastrophic failure because of improper monitoring and maintenance (Som *et al.* 2019). The SHM involves creating an undamaged response model of the structure in its undamaged state and comparing the same response with the future response. This comparison can be made on the static as well as vibrational structural responses (Farrar *et al.* 2001, Wu and Smyth 2007). However, the collection of undamaged responses becomes a barrier for the SHM of existing structures as these structures

*Corresponding author, Ph.D., E-mail: gmondal@iitbbs.ac.in

^aM.Tech

^bPh.D.

^cPh.D.

may have some pre-existing damages.

In this study, a damage detection approach is presented for old and existing structures in which the initial design properties are used for damage detection. The approach consists of three steps; first, the collection of experimental modal parameters of the damaged structure, second, creation of a FE model of structures using its initial design properties, and third, tuning of FE model to match experimental response. The choice of optimization tool and objective functions have been presented here. The study involves both numerical and experimental validation of the approach.

2. State-of-the-art review of literature on the damage detection technique

Several methods are available in the literature to solve the damage detection problems in the absence of an undamaged state response. These include wave propagation (Qiao and Fan 2014), electrical resistance tomography (Smyl *et al.* 2018), the transmissibility of responses (Schallhorn and Rahmatalla 2015), and probabilistic approaches (Ching *et al.* 2006). However, these methods are useful for local damage detections. For global damage detection, the use of data-driven approaches such as machine learning techniques, and artificial neural networks (Nguyen *et al.* 2018) are also prevalent in practice. However, these data-driven techniques require extensive data training, high computational efficiency and are dependent on data handling rather than actual structural behaviour. There are many probabilistic methods available for SHM (Beck 2010), including the Bayesian method of finite element model updating (Ching *et al.* 2006, Erazo and Nagarajaiah 2017, Sun and Büyüköztürk 2016, Behmanesh *et al.* 2015). This method uses Bay's theorem of probability to update the parameters of the finite element model, and studies have been done to apply this method in large-scale civil engineering structures (Behmanesh and Moaveni 2015, Erazo *et al.* 2019). The finite element (FE) model updating technique (Stubbs and Kim 1996, Moaveni *et al.* 2008, Jaiswal *et al.* 2020), also known as the inverse approach of modelling, overcomes the problems associated with other approaches in existing structures. This method involves updating the FE model iteratively to achieve a structural response that matches with the same collected experimentally. The complete model updating technique consists of three critical parts, i.e., the objective function (OF) to be minimized, the optimization tool, and the structural analysis tool, which are reviewed below.

Amongst various objective functions, the modal response based objective functions are most widely used, as the cracks and damages alter the vibrational properties of the structure (Azim *et al.* 2020, Razavi and Hadidi 2020). These objective functions can be written in the form of frequency (Khatir *et al.* 2018), mode shape (Mishra *et al.* 2020), strain energy (Meruane and Heylen 2011), modal strain energy (Arefi and Gholizad 2020), FRF (Mohan *et al.* 2013), and sometimes a combination of frequency and mode shapes (Moaveni *et al.* 2010, Jafarkhani and Masri 2011, Jaiswal *et al.* 2020).

Several optimization algorithms are available in the literature to solve the inverse-based damage identification problem. For example, the Genetic Algorithm (Meruane and Heylen 2011), the Particle Swarm Optimization (PSO) (Mohan *et al.* 2013), the CMA-ES Optimization (Jafarkhani and Masri 2011), Ant Lion Optimization (ALO) (Mishra *et al.* 2019), the Teaching–Learning-Based Optimization (TLBO) (Rao *et al.* 2011, 2012, Khatir *et al.* 2019), and many others for better convergence (Kaveh and Zolghadr 2017, Varma *et al.* 2020). Some comparative studies among these algorithms have also been performed (Fowler *et al.* 2008, Mishra *et al.* 2020).

Stubbs and Kim (1996) presented a methodology for damage detection by creating a baseline

model in a FE software of a damaged structure. Two span continuous aluminium beam is considered as test specimen with increasing damage intensity at one location. Beam like structures have been a general structural configuration used in the literature to validate any proposed damage detection technique (Moaveni *et al.* 2008, Khatir *et al.* 2018, Mishra *et al.* 2019). These model updating techniques require programmable software for the iterative updating of the FE model (Dinh-cong *et al.* 2020). However, they rely on the use of costly commercial software for numerical modelling and optimization algorithm. Furthermore, some of the major limitations in the model updating techniques currently used are listed below:

- (i) Modelling full-scale complex structures using a computational program is not only challenging but also time-consuming. It also may not reflect the actual behaviour of the structures due to modelling simplifications (Jin and Jung 2016), such as; the nonlinearity of connections, soil-structure interaction, non-structural systems, hydrodynamic interactions, mass distribution in the structure, etc.” The entire damage detection process is dependent on the efficacy of the used optimization algorithm and the structural analysis software; such optimization algorithms and software are costly and require high computational efficiency. Furthermore, many of the optimization algorithms mentioned above prematurely converge to local minima and cannot identify damages.
- (ii) Literature has focused on the use of damage vectors for indicating damage in an element (Mishra *et al.* 2019, Dinh-cong *et al.* 2020). These vectors can identify a percentage decrease in the stiffness of an element. But in reality, damage not necessarily reduces the stiffness of a zone; it may increase the stiffness, as can be seen in bearings of bridges, blockage of expansion joints, additional patchwork, etc.
- (iii) Most of the past studies focused on numerical validations instead of experimental verifications.

Therefore, the present study proposes a damage detection technique for existing structures using two open source codes. The effectiveness and robustness of the technique proposed are investigated through a cantilever beam and a fixed beam, both experimentally and numerically. Here, the focus is mainly on the proposed technique development and validation, as it is necessary to check its performance in a simple structure before applying it to large-scale real-life complex structures.

3. Damage detection methodology

The methodology in the current study involves a finite element (FE) model updating technique, popularly known as the inverse approach. The structural model is compared and updated in this method based on the recorded actual structural response (Zanardo *et al.* 2006). The methodology broadly contains two parts; the collection of actual structural responses through the experiment, and the numerical model updating (Fig. 1). The model updating consists of three major components, (a) the numerical analysis of the structure, (b) error calculation by using an objective function, and (c) optimization. In the present study, an open-source code OpenSees[®] 3.1.0 (McKenna 2011), is used for numerical modelling the structure and updating. This code provides simple structural modelling, modification, model updating and simulations, and can be modified by the user as per the requirement. Furthermore, an open-source optimization tool, NOMAD[®] 3.9 optimization (Audet and Dennis 2006), is used to update the damage parameter in the FE model created in OpenSees to minimize the objective function. NOMAD being a derivative-free

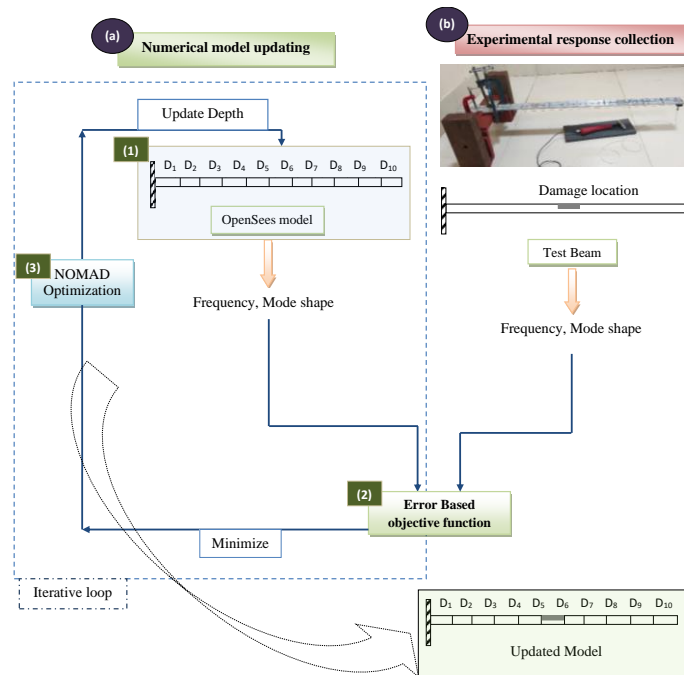


Fig. 1 Flowchart of the damage detection methodology

optimization method overcomes the limitations of the optimization algorithms mentioned above. NOMAD calls OpenSees and control the updating parameter iteratively, keeping a goal to minimize the objective function value. The methodology is applied to a cantilever beam and a fixed beam.

The numerical model of the beam is prepared using two-noded, linear-elastic beam-column elements and divided into several finite elements. Since the presence of damage in an element alters the stiffness, and thus the structure's natural frequency, the stiffness can be assumed as a damage indicating parameter. Also, variation in mass after damage has opposite effects in the natural frequency. This can be captured by exclusively modelling the same. Hence, the depth of the beam is taken as the damage indicating parameters in the present study as it is directly related to the stiffness via the moment of inertia and the mass via density. Therefore, the depth of each element is considered as a variable keeping other structural properties constant. This can capture the changes in modal properties due to variation of stiffness as well as mass. Thus, the number of variables is the same as that of finite elements (FEs) in the model. During the updating process, the depth of each FE is provided as input by the optimization tool. The numerical model is updated and analyzed for a set of depths provided by the optimization tool to obtain the modal responses which are used to evaluate the objective function.

The choice of the objective function is critical and affects the successful model updating process and, thus, damage detection. Amongst the various objective functions (OF) available in the literature, the frequency and mode shape-based OF are chosen here because these are the fundamental dynamic properties of a structure and are easy to extract. The natural frequencies are a global indicator of the structural state, whereas vibrational mode shapes provide more local data. Two objective functions, one considering natural frequency (Khatir *et al.* 2018), another a

combination of frequency and mode shape (Jafarkhani and Masri 2011) are chosen here (Jaiswal *et al.* 2020), as shown in Eqs. (1) and (2), respectively. The effect of mode shapes is represented by modal assurance criteria (MAC) value, as shown in Eq. (3), which is a simple and most widely acceptable parameter to compare mode shapes (Pastor *et al.* 2012). MAC is a scalar number that varies from 0 to 1, where a MAC value close to 1 represents more similarity between two mode shapes.

$$OF_{*1} = \sum_{i=1}^N \left(\frac{f_i^{nu} - f_i^{ex}}{f_i^{ex}} \right)^2 \quad (1)$$

$$OF_* = \sum_{i=1}^N \left(\frac{f_i^{nu} - f_i^{ex}}{f_i^{ex}} \right)^2 + \sum_{i=1}^N (1 - MAC_{ii}) \quad (2)$$

$$MAC_{ii} = \frac{|\phi_i^{nuT} \cdot \phi_i^{ex}|^2}{(\phi_i^{nu} \cdot \phi_i^{nu})(\phi_i^{ex} \cdot \phi_i^{ex})} \quad (3)$$

Where, f^{nu} and f^{ex} are numerical and experimental frequency of the structure, respectively, N is the number of modes considered, ϕ^{nu} and ϕ^{ex} are normalized numerical and experimental mode shapes, respectively. These objective functions represent the difference between numerical and experimental responses in the form of a scalar number.

The basic parameters for NOMAD optimization are the number of variables, values of the variable (initial, upper bound, and lower bound), and the function evaluation limit. The number of variables is equal to the number of FEs considered in the numerical model in OpenSees. Values of variables can be decided based on the severity of damage and possible deviation from the mean initial depth. The function evaluation limit is decided based on the required degree of accuracy. Optimization starts with the given initial set of depths as variables. After the modal analysis of the numerical model, the OF value is evaluated for the set of variables. The evaluated value of OF becomes the final single output from the updating model, which is an input for the optimization tool. By observing the input OF value, the optimization tool creates a new set of depths for each element for the subsequent evaluation and updates the model. During each consecutive iterations, NOMAD updates the numerical model several times and tries to get a converged set of depth values for which the objective function evaluation is minimum. This complete process runs iteratively to minimize the OF value and achieve a best-converged solution. A representation of the proposed methodology is shown in Fig. 1. Once the numerical model is updated and optimized satisfactorily, it will replicate the depth/stiffness scenario of the actual structure.

3.1 Optimization tool

Nonlinear Optimization with Mesh Adaptive Direct-Search (NOMAD) algorithm is a derivate-free method that uses direct search function evaluation in the space of variables and hence can deal with missing function values (Audet and Dennis 2006, Le 2011). In the present study, OpenSees is the blackbox program that uses input values from NOMAD to minimize the output function. NOMAD has been already used and found effective in several studies and optimization problems in many fields, such as mechanical design problems (Bahrami *et al.* 2016), radiation, and particle

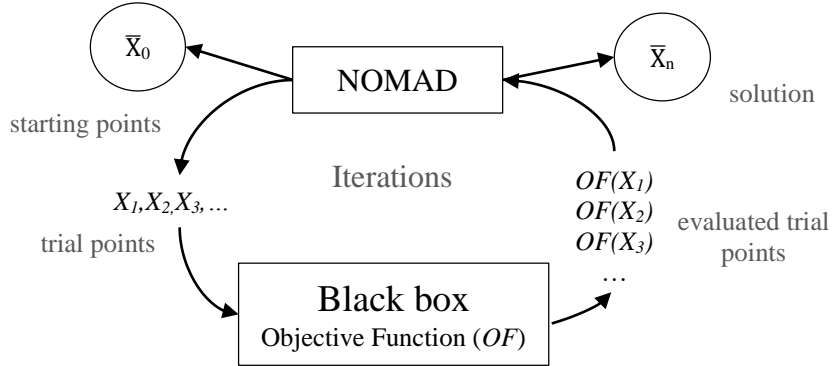


Fig. 2 An optimization link between NOMAD and the blackbox problem

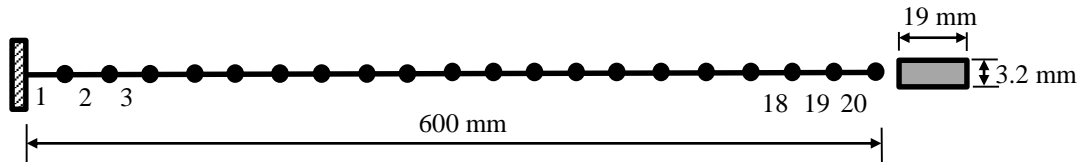


Fig. 3 Cantilever beam model

tracking problems (Dubé *et al.* 2014). Fig. 2 shows a general working principle of NOMAD or any direct search method. The NOMAD iteratively constructs a list of trial points that OpenSees evaluates. A more detailed study on the algorithm and working principle of NOMAD optimization can be found elsewhere (Zanardo *et al.* 2006, Audet and Dennis 2006, Audet and Hare 2017).

4. Numerical modelling

The proposed damage detection methodology is applied to a cantilever steel beam. For this purpose, a numerical FE model of the steel cantilever beam is prepared in OpenSees (Fig. 3). The dimensions of the beam are $0.6 \text{ m} \times 0.019 \text{ m} \times 0.0032 \text{ m}$, having a mass density of 7717.61 kg/m^3 and modulus of elasticity 207 GPa. The beam is initially modeled with twenty numbers of two-noded, linear-elastic beam-column elements. Beam modelling is considered in 2-D space with three degrees of freedom (3 DOF) at each node. Here, the depth of each element is kept as a variable, as discussed in section 3. The dynamic responses, i.e., natural frequency and mode shape vector of the beam, are obtained using the eigenvalue solver command in OpenSees. It is to be noted that the experimental response is a constant parameter in the objective function, while the numerical response changes in each iteration based on the variables provided by the NOMAD.

4.1 Selection of objective function

Damage detection by optimization is greatly dependent on the choice of the objective function to be minimized. In this study, initially, the frequency-based objective function (Eq. (1)) proposed by Khatir *et al.* (2018) is used. These objective functions give higher weightage to fundamental

Table 1 Numerical cases for objective function selection

Objective function	OF_{*1}				OF^*
	Case 1		Case 2		
Number of elements	10	10	10	20	20
Considered number of modes	10	9	8	10	6
Depth of elements (mm)	3.2	3.2	3.2	3.2	3.2
Initial depth (mm)	2.5	2.5	2.5	1	3
Upper bound of depth (mm)	4	4	4	3.2	4.2
Lower bound of depth (mm)	1	1	1	2.5	1.8
Number of function evaluations	5000	5000	5000	10000	10000
Obtained average error per element (%)	0.15	24	33	8.25	0.05

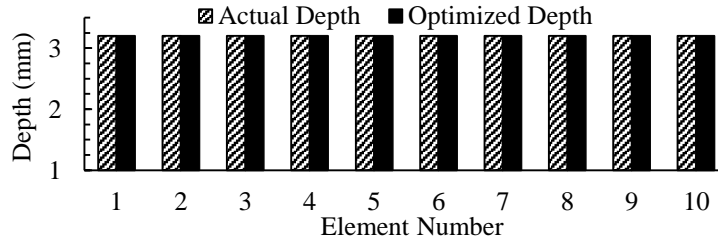


Fig. 4 Optimization result with 10 number of elements considering OF*1

frequencies when a higher power frequency term is present in the denominator. Initially, the numerical model of the cantilever beam is considered with ten elements and termed as case 1. The considered optimization parameters for this case are shown in Table 1. The first ten frequency responses are recorded and are used to update the undamaged state of the beam. The obtained optimized depth result after a total of 3351 function evaluations is shown in Fig. 4. The obtained average percentage error considering error in each element for frequency-based objective functions calculated from Eq. (4) is 0.15%.

$$Error = \sum_{i=1}^n \left(\frac{|AD - OD|}{AD} \times 100 \right) \div n \tag{4}$$

Where *Error* refers to the average percentage error per element between actual and updated depth, *AD* refers to the actual depth, *OD* refers to the optimized depth, and *n* is the number of elements. Furthermore, reduction in the number of modes leads to increase in error. The objective function OF_{*1} given by Khatir *et al.* (2018) shows better results close to the actual depth of 3.2 mm when higher modes are considered.

The objective function OF_{*1} is again checked for efficiency by increasing the number of elements, changing the bound values with increased function evaluations limit, case 2 (Table 1). The obtained optimized depth result after 9480 function evaluations is shown in Fig. 5. The average percentage error in each element is found to be 8.25% (Eq. (4)).

It is seen that, as the number of elements is increasing, the error in optimization results is

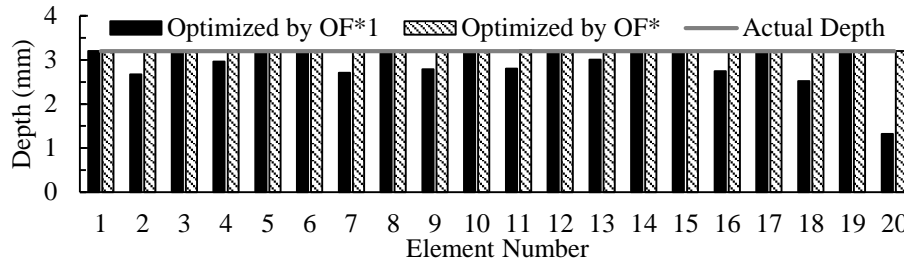


Fig. 5 Optimized depth result with 20 elements considering OF*1 and OF*

increasing. Since the effect of individual elements in the global frequency response of the beam is decreased. Also, two structures with different stiffness configurations may have the same frequency of vibration. Hence, it is concluded that the natural frequency alone cannot be used to detect damage intensities, especially in the case of complex damage conditions with fewer modes. But it can be used for quick and broad identification of damage zones, considering higher modes in the optimization, although it is difficult to extract the higher modes of any structure experimentally.

Therefore, an objective function OF^* (Eq. (2)) proposed by Jafarkhani and Masri (2011) is used here. This objective function uses the effect of mode shapes, added in the form of MAC value and frequency. Optimization is performed on the beam with twenty elements considering only six modes (Table 1), and the obtained results are shown in Fig. 5. The result shows that the addition of the effect of mode shapes makes a unique configuration of the structure and significantly enhances the optimization results. Further, the performance of OF^* is compared with that of the other available forms of combined frequency and mode shape-based objective function in section 6.2. It has been observed that the OF^* performed better than other objective functions.

4.2 Study on an adequate number of modes required for the inverse approach

In this study, starting from 1st mode to up to the initial ten modes of responses is considered for optimization to know the minimum number of modes required for the adequate performance of the proposed method (modified from Jaiswal *et al.* 2020). Here, undamaged state (i.e., 3.2 mm uniform depth in all elements) numerical response of cantilever beam is collected, and the same is taken as reference response to obtain back the same uniform depth via the inverse approach of model updating. The optimization parameters considered are upper bound, lower bound, and initial depth as 4.2 mm, 1.8 mm, and 3 mm, respectively, assuming a 40% deviation from the mean value. The number of function evaluations is limited to 10000.

Fig. 6 shows the average percentage error (Eq. (4)) obtained and function evaluations considered for the optimization with an increasing number of modes. The error is decreasing as the number of modes considered in the objective function increases, so the accuracy is increasing. Also, as the number of modes increases, the optimization is converging fast, taking fewer function evaluations, hence lesser computational time (here, the function evaluations limit is kept to 10000).

The required number of modes can be fixed depending on the damage severity, structural importance, and accuracy of extracted experimental response. It is recommended to consider at least five modes to avoid the occurrence of false damage detection. In the current study, six modes are considered for the further damage detection process.

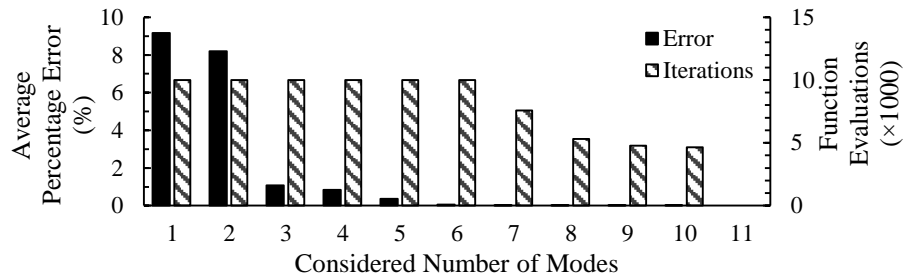


Fig. 6 Sensitivity analysis for the number of modes consideration in model updating

Table 2 Numerical damage cases listed with reduced element depths

Damage case	Case 1	Case 2	Case 3
Number of elements	20	20	30
Damaged element number	10	6	14
Depth of damaged element (mm)	2	2	2
Depth of remaining element (mm)	3.2	3.2	3.2
Initial depth (mm)	3.0	3.0	3.0
Upper bound of depth (mm)	4.2	4.2	4.6
Lower bound of depth (mm)	1.8	1.8	1.4
Number of function evaluations	20000	20000	30000

5. Numerical verification of the proposed scheme

Three numerical damage cases have been considered in the form of a reduction in the depth of several elements, as shown in Table 2. The optimization parameters are shown in Table 2, where the bound values are considered assuming a 40% deviation of depth from the mean value in damage cases 1 and 2. And assuming a 60% deviation in damage case 3. Also, to increase the complexity of damage detection, the number of elements is increased from 20 elements to 30 elements for the third damage case.

Table 3 shows obtained natural frequency and mode shapes of the cantilever with these damage cases for up to the initial six modes. Here, the percentage change in frequency in the presence of damage is shown; here negative sign denotes a reduction in frequency value. These damaged beam responses are taken for optimization to identify the known damages for all three cases. The obtained optimized depths showing damage locations and intensities are shown in Figs. 7-9. It is observed that the proposed methodology can identify the damage location at the same time, the intensities very accurately. In case 3 (Fig. 9), with multiple damages with different intensities, the method can locate all these damages along with the intensities. For the first two damage cases, optimization converged at 10928 and 11319 function evaluations, respectively. Whereas, for case 3, full 30000 function evaluations are exhausted, which indicates that there is further scope of refinement of optimized depth results to obtain more accurate value, if function evaluations limits are set to increase.

In order to replicate a practical scenario where noise can be present in the recorded data, a small noise of 0.5% for frequency and 5% for mode shapes are considered in the present study

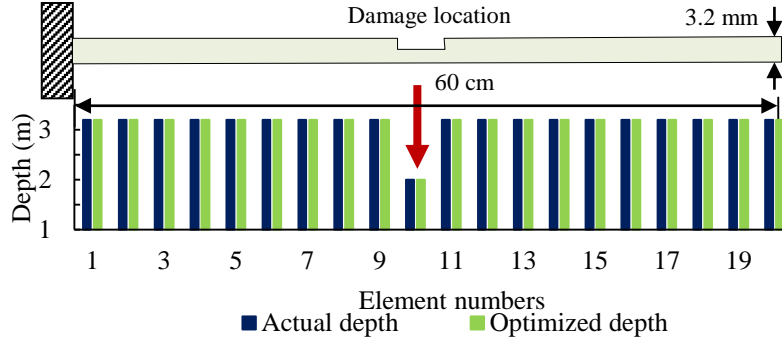


Fig. 7 Comparison of actual and optimized depths for different damage cases Case 1: Single damage

Table 3 Obtained natural frequencies for different damage cases in the cantilever beam

Mode	Natural frequency (Hz)						
	Undamage case	Damage cases					
		Case 1	% Change	Case 2	% Change	Case 3	% Change
1 st	7.43	7.15	-3.77	6.70	-9.83	6.41	-13.73
2 nd	46.52	42.02	-9.48	42.59	-8.25	38.08	-18.14
3 rd	130.11	129.19	-0.35	109.81	-15.30	112.88	-13.24
4 th	254.67	235.52	-7.05	239.48	-5.49	206.17	-19.04
5 th	420.50	412.09	-1.35	402.43	-3.66	331.82	-21.09
6 th	627.41	592.01	-4.87	568.85	-8.59	538.28	-14.21

following Mishra *et al.* (2020) and Majumdar *et al.* (2014), given by Eqs. (5) and (6) The results found from the noise-free data are acceptable with reference to the results from noisy data, as can be seen in Fig. 9. Therefore the further numerical study is conducted using noise-free data.

$$f_{noise} = f_{analytical} \left(1 + \frac{rand(-1,1) \times \delta}{100} \right) \quad (5)$$

$$\phi_{noise} = \phi_{analytical} \left(1 + \frac{rand(-1,1) \times \delta}{100} \right) \quad (6)$$

5.1 Comparative study

The efficiency of NOMAD optimization for the application of damage identification is compared with two of the commonly used damage detection algorithms, i.e., ALO (Mirjalili 2015) and TLBO (Rao *et al.* 2011, 2012). Multiple damage case as discussed in the above section is considered for the purpose of comparison. Using ALO, TLBO, and NOMAD, the best results with their minimal objective function value are obtained after 140000, 340000, and 30000 number of function evaluations (NOFs), respectively. The depth values obtained and the convergence curve

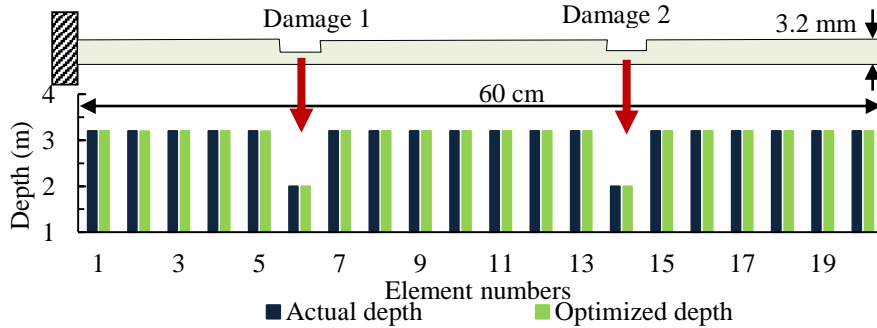


Fig. 8 Comparison of actual and optimized depths for Case 2: Double damage

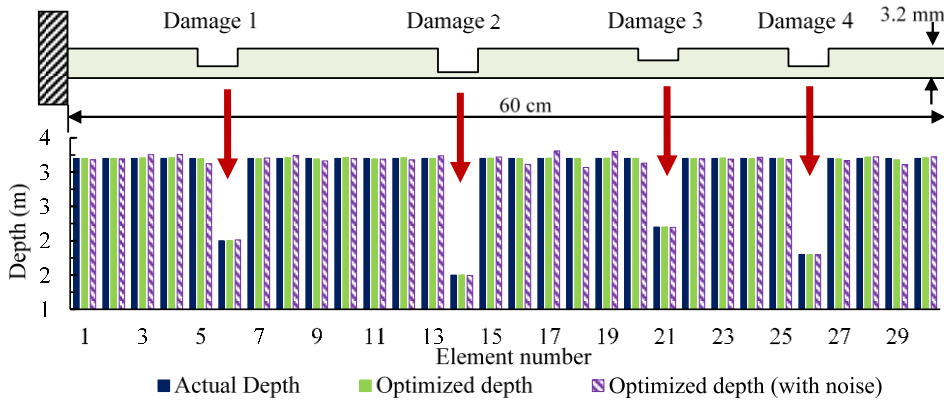


Fig. 9 Comparison of actual and optimized depths for Case 3: Multiple damages

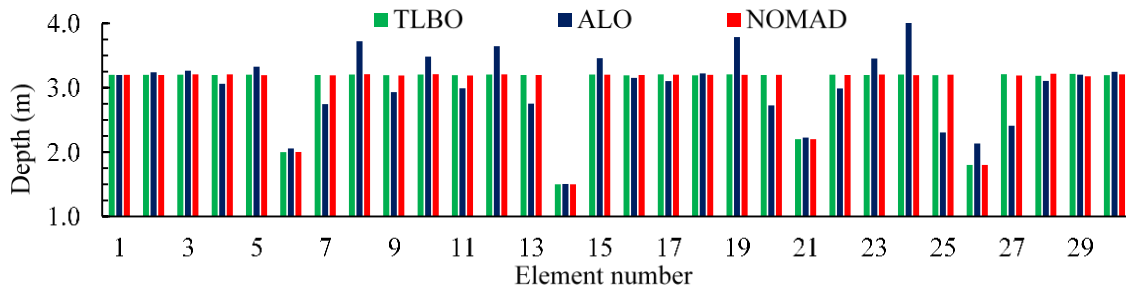


Fig. 10 Comparison of optimized depth obtained using different algorithms

by using three algorithms are shown in Figs. 10 and 11, respectively. It is observed that by using ALO converged to a local minima, the optimized depth obtained is near to expected but still has chances of better results. The ultimate results of TLBO and NOMAD results are very similar and exact but, NOMAD requires less function evaluation than TLBO. From the results, it is concluded that the performance of NOMAD is consistent with commonly used optimization algorithms. For more comparative study and advantages of using NOMAD over other algorithms, the reader can refer to Fowler *et al.* (2008), Rios and Sahinidis (2010) and Le Digabel (2011).

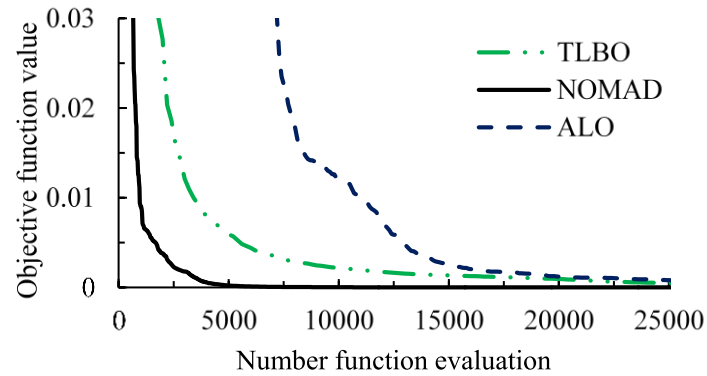


Fig. 11 Convergence curve for multiple-damaged cantilever beam problem

Table 4 Numerical minor damage cases listed with reduced element depths

Parameters	Damage cases	
	Case A (5% damage in one element)	Case B (5% damage in one element and 10% damage in another element)
Number of elements	20	20
Damaged element number	5	5
Depth of damaged element (mm)	3.04	3.04
Depth of remaining elements	3.2	3.2
Initial depth	3.0	3.0
Upper bound of depth	4.2	4.2
Lower bound of depth	1.8	1.8
Number of function evaluations	20000	20000

5.2 Minor damage case

In this section, small damages of 5% and 10% depth reduction have been considered numerically to see the effectiveness of the method to detect small damage. The damage cases, their intensities, and considered optimization parameters are tabulated in Table 4 and obtained damaged beam frequency response are shown in Table 5. The obtained optimization results are shown in Fig. 12. From the obtained results of optimized depths, it is seen that even small damages of 5% and 10% can be effectively identified, as shown in red bars in the plots. The actual damaged depth of elements 5 and 14 was 3.04 mm and 2,88 mm, respectively, and the same is obtained after optimization. The method can identify finer damages with their exact locations and intensities.

6. Experimental verification of the proposed scheme

An aluminum cantilever beam of cross-section 50 mm × 5 mm, length 80 cm, and the modulus

Table 5 Obtained natural frequencies with minor damage cases

Mode	Frequency (Hz)				
	Undamaged case	Damaged cases			
		Case A	% Change	Case B	% Change
1 st	7.43	7.37	-0.81	7.39	-0.54
2 nd	46.52	46.45	-0.15	45.96	-1.20
3 rd	130.11	129.42	-0.53	127.55	-1.97
4 th	254.67	252.33	-0.92	251.91	-1.08
5 th	420.50	416.85	-0.87	414.73	-1.37
6 th	627.41	622.27	-0.82	615.58	-1.89

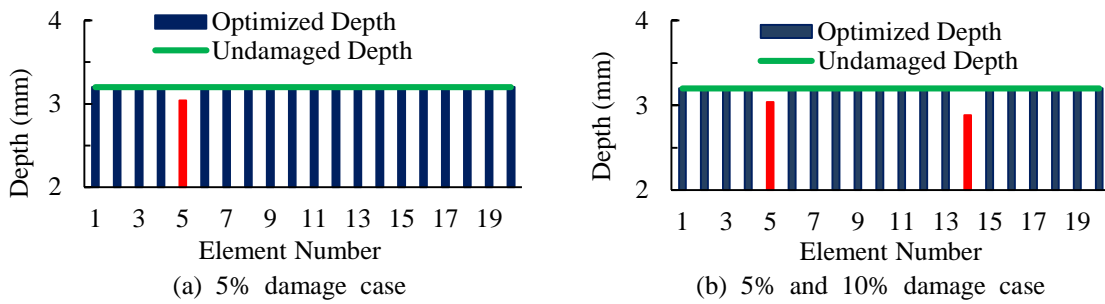


Fig. 12 Optimized depth results for smaller damage intensity

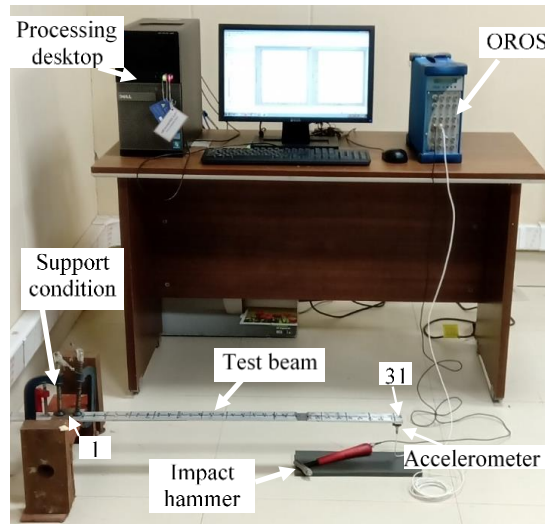


Fig. 13 Experimental setup of modal impact hammer test

of elasticity 69 GPa is chosen to validate the approach proposed here experimentally. The beam's experimental natural frequency and mode shape are extracted using the modal impact hammer test (Fig. 13). The beam is divided into 30 elements, and a roving impact hammer test is performed,

Table 6 Experimental damage cases and optimization parameters

Damage case	Single damage	Double damage	
Number of elements	30	30	
Damaged element number	21 st	7 th	21 st
Depth of damaged element (mm)	2.37	3.06	2.37
Depth of remaining undamaged element (mm)	5	5	
Initial depth (mm)	5.0	5.0	
Upper bound of depth (mm)	8.0	8.0	
Lower bound of depth (mm)	2.0	2.0	
Number of function evaluations	30000	30000	

and the acceleration is recorded using an accelerometer attached at the free end. The frequency response function (FRF) of the force at all 31 nodes and response at the free endpoint, i.e., 31st node, is obtained using OROS Analyser (Fig. 13). No filter is applied for obtaining FRFs at each node.

An FRF is a function which shows the structural response for an applied force, both in the frequency domain, as given by Eq. (7).

$$H(w) = \frac{A(w)}{F(w)} \quad (7)$$

Where $H(w)$ the FRF, $F(w)$ is the external force, and $A(w)$ is acceleration response; all are in the frequency domain. After the collection of FRFs for all the 31 nodes, the FRF data block is imported into ME'Scope VES[®] v5.1, and curve fitting is carried out to obtain the natural frequency and mode shapes of the beam. This method is giving acceptable accuracy in obtaining frequency and mode shape in the current test specimen.

6.1 Single damage cases

Predefined damage cases are considered by reducing the depth of elements, as tabulated in Table 6. The damage in an element is made using an angle grinder and filing equipment, and reduced average depth is measured using a micrometer. The damage in the 21st element is shown in Fig. 14. A roving impact hammer test is conducted over the damaged beam with a soft hammer tip. As an example, Fig. 15 presents different plots obtained after each hammering.

The experimentally obtained natural frequencies of the first six modes for case 1 are tabulated in Table 7 and the corresponding mode shapes are shown in Fig. 16. These mode shapes and natural frequencies (column D in Table 7) are taken for model updating with optimization parameters tabulated in Table 6. The result can be seen in Fig. 17, obtained for the optimized depth of each element after 16813 function evaluations and around 68 minutes of computational time. It can be seen from Fig. 17 that the proposed approach can adequately identify the damaged location and the intensity at the 21st element. There are some false depths identified because of the noise present in the experimental response. The calculated error between optimized and actual depth is found to be 13.25% (Eq. (4)).

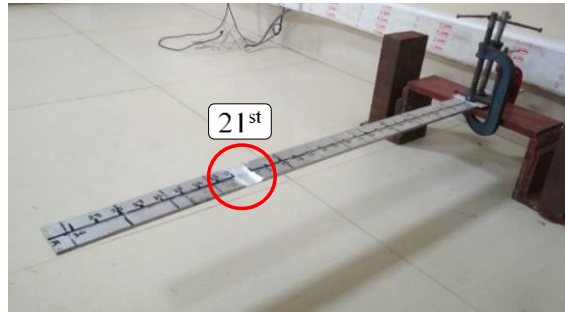


Fig. 14 Single damage 50% depth reduction at 21st element

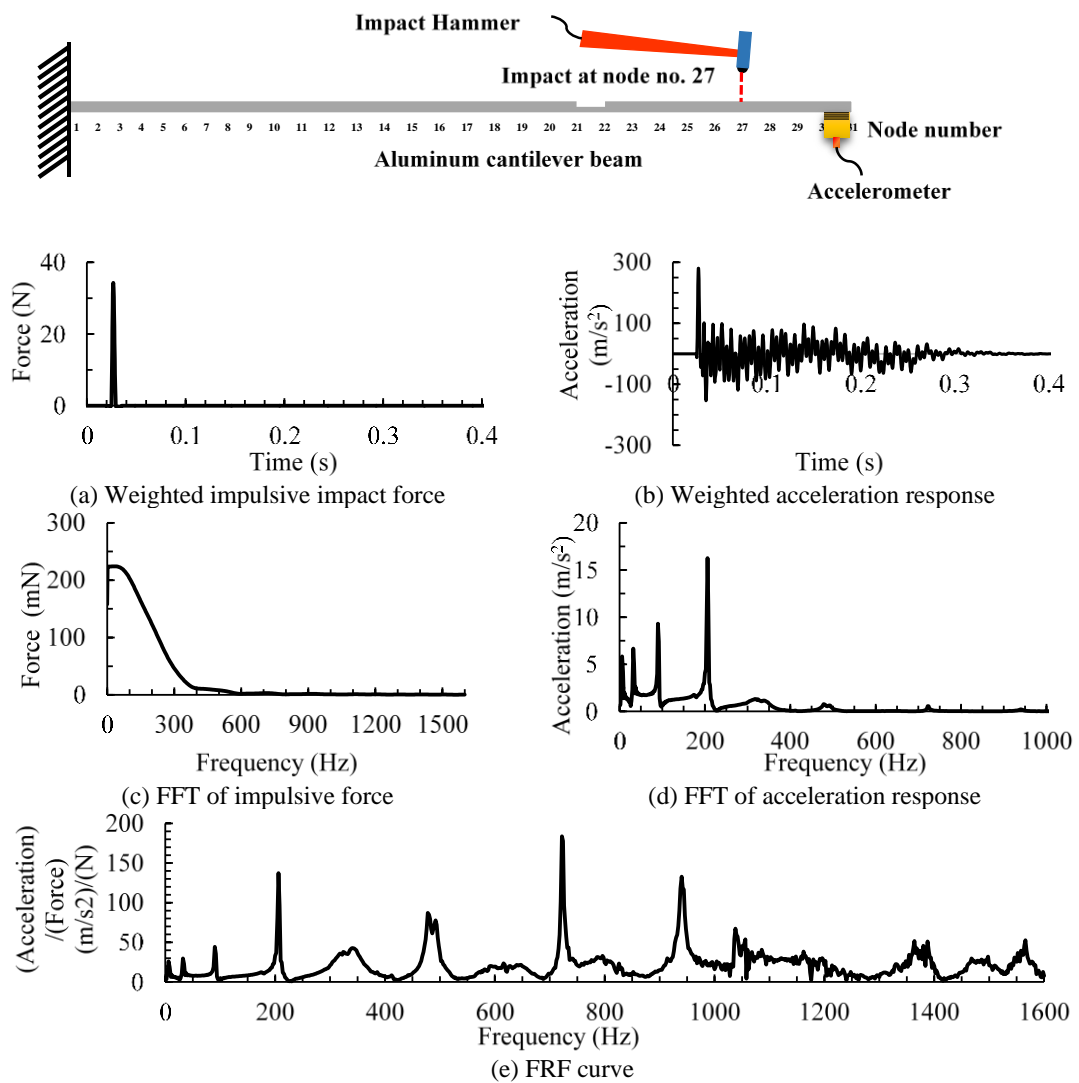


Fig. 15 Plots showing the collected responses at 31st node, impact at 27th node

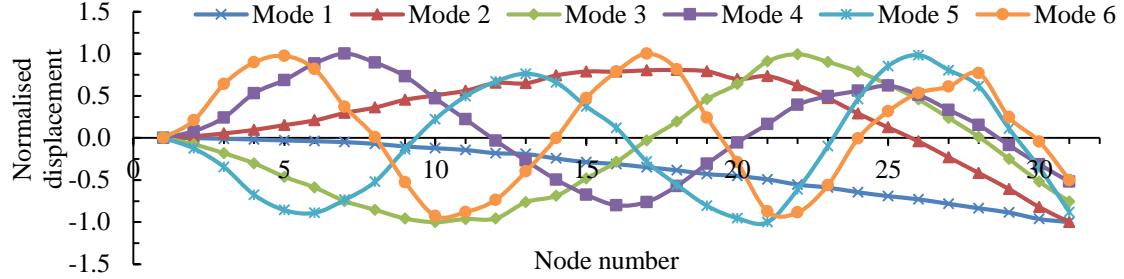


Fig. 16 Normalized experimental mode shapes of the aluminum cantilever beam

Table 7 Single damage case: Comparison of natural frequencies (Hz), (Num – Numerical, Exp-Experimental)

Modes	Undamaged			Damaged			Percentage change	
	Num	Exp	% Error	Num	Exp	% Error	Num	Exp
	[A]	[B]	$\frac{(A - B) \times 100}{A}$	[C]	[D]	$\frac{(C - D) \times 100}{C}$	$\frac{(C - A) \times 100}{A}$	$\frac{(D - B) \times 100}{B}$
1	6.28	6.06	3.50	6.27	5.96	4.94	-0.16	-1.65
2	39.3	37.8	3.82	33.95	31.7	6.63	-13.61	-16.14
3	109.93	107	2.67	93.38	90.4	3.19	-15.06	-15.51
4	215.17	209	2.87	210.04	207	1.45	-2.38	-0.96
5	355.27	358	-0.77	342.68	337	1.66	-3.54	-5.87
6	530.07	531	-0.18	486.01	485	0.21	-8.31	-8.66

The accelerometer attached at the free end of the cantilever beam and its thick supporting mold cause resistance to vibration and show comparatively higher stiffness in the end zone. Its weight is about 3% than that of the beam and about 86% than that of each element. Hence, the end elements are showing false damage. The self-weight of the accelerometer and mold is significant compared to the weight of each element. It is expected that the effects of instrument attachments will not be significant in stiffer and bigger structures.

6.2 Comparison of different choices of objective functions

The result obtained here using the objective function in Eq. (2) (Jafarkhani and Masri 2011) for the single damage case is compared further with other available objective functions in the literature, which considers both natural frequency and the mode shape. OF_1 (Meruane and Heylen 2011), OF_2 (Barman *et al.* 2020), OF_3 (Jin *et al.* 2014), OF_4 (Mishra *et al.* 2019) and OF_5 (Modified Dong-Cong *et al.* 2020) are shown in the Eqs. (8)-(12).

$$OF_1 = \sum_{i=1}^N \left(\frac{f_{inu}^2}{f_{iex}^2} - 1 \right)^2 + \sum_{i=1}^N (1 - MAC_{ii})^2 \quad (8)$$

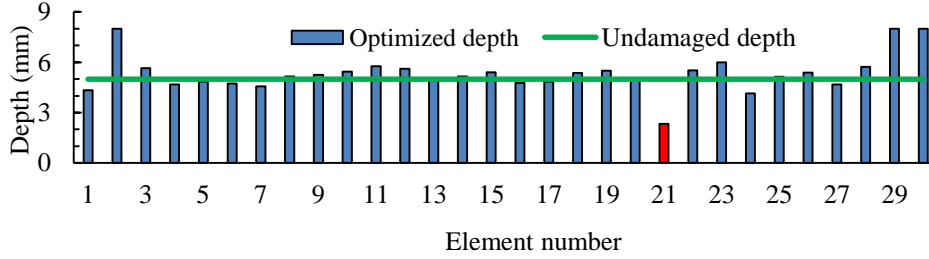


Fig. 17 Optimized depth comparison for single damage case

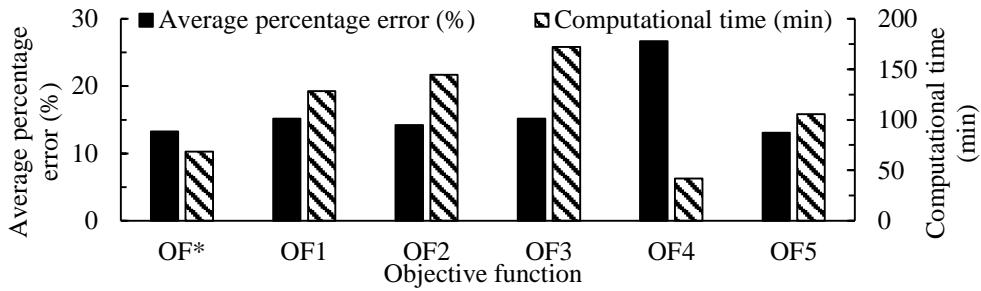


Fig. 18 Objective function comparison considering the case of the experimental response

$$OF_2 = \sqrt{\frac{1}{N} \sum_{i=1}^N \left(\frac{f_i^{ex}}{f_i^{nu}} - 1 \right)^2} + \sum_{i=1}^N (1 - MAC_{ii}) \quad (9)$$

$$OF_3 = \sum_{i=1}^N \left[\frac{f_i^{nu} - f_i^{ex}}{f_i^{ex}} \right]^2 + \sum_{i=1}^N \left[\frac{(1 - \sqrt{MAC_{ii}})^2}{MAC_{ii}} \right] \quad (10)$$

$$OF_4 = \sqrt{\frac{1}{N} \sum_{i=1}^N (f_i^{nu} - f_i^{ex})^2} + \sum_{i=1}^N (1 - MAC_{ii}) \quad (11)$$

$$OF_5 = \sum_{i=1}^N \left(\frac{f_i^{nu} - f_i^{ex}}{f_i^{ex}} \right)^2 + \sum_{i=1}^N (1 - \sqrt{MAC_{ii}}) \quad (12)$$

The optimization parameters, i.e., lower bound, upper bound, initial depth, and function evaluations limit, are kept the same as 2 mm, 8 mm, 5 mm, and 30000, respectively. The plot showing the average percentage error in each element from each objective function is presented in Fig. 18. The average percentage error in each element is the least in the case of OF* and OF5. Additionally, OF* is taking the least computational time along with satisfactory results, as reported in Fig. 18.

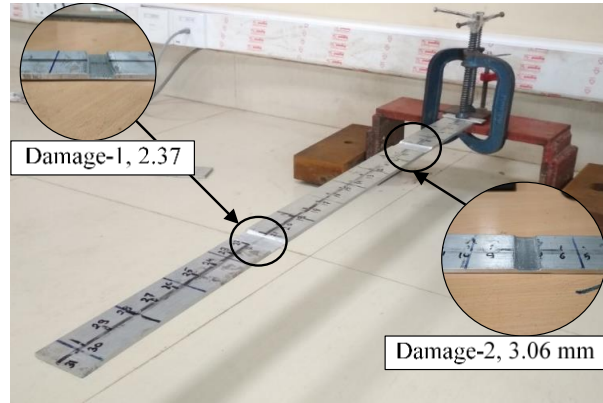


Fig. 19 Cantilever beam with two damage cases at 21st and 7th element number

Table 8 Double damage case: Comparison of natural frequencies (Hz), (Num – Numerical, Exp-Experimental)

Modes	Undamaged			Double damage case			Percentage change after damage	
	Num	Exp	% Error	Num	Exp	% Error	Num	Exp
	[A]	[B]	$\frac{(A - B) \times 100}{A}$	[C]	[D]	$\frac{(C - D) \times 100}{C}$	$\frac{(C - A) \times 100}{A}$	$\frac{(D - B) \times 100}{B}$
1	6.28	6.06	3.50	5.69	5.3	6.85	-9.39	-12.54
2	39.3	37.8	3.82	33.97	32.4	4.62	-13.56	-14.29
3	109.93	107	2.67	91.51	88.1	3.73	-16.76	-17.66
4	215.17	209	2.87	197.75	191	3.41	-8.10	-8.61
5	355.27	358	-0.77	334.78	337	-0.66	-5.77	-5.87
6	530.07	531	-0.18	482.65	482	0.13	-8.95	-9.23

6.3 Double damage case

Another damage with a different damage intensity in the same cantilever beam with single damage is introduced on the 7th element. The average reduced depth is measured as 3.06 mm (Fig. 19). Similar to the previous case, the modal impact hammer test is repeated on the beam to obtain experimental vibrational response. Frequencies and mode shapes obtained are then used for the optimization with the objective function OF^* (Table 6). Table 8 presents the obtained experimental and numerical natural frequencies. Some deviations in the expected experimental response is because of noise and improper fixity at the beam end. The optimized depth result can be seen in Fig. 20. Both the damages are identified with their adequate locations at the 21st and the 7th elements, as shown in red color bars in the graph. Similar to the first case, there are some false depths identified as the increased depth. The calculated average error per element, compared between optimized and actual depth here using Eq. (4), is 13.5%. It can be observed that the accuracy of identification will entirely depend on the accuracy and perfection of the extracted experimental response.

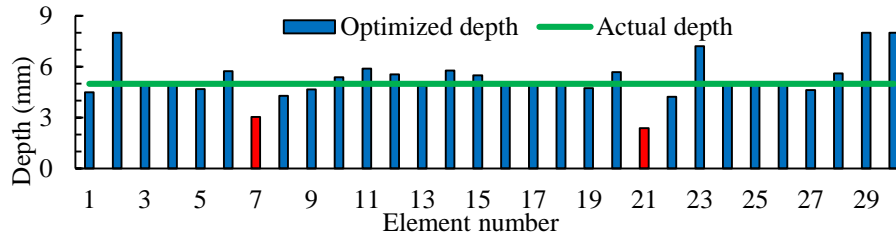


Fig. 20 Optimized depth comparison for double damage case

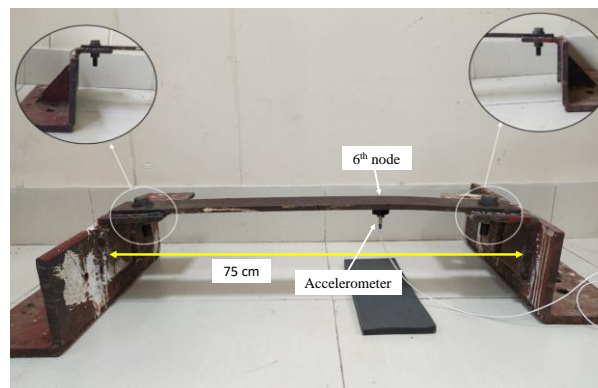


Fig. 21 Fixed beam structure with 15 divisions and 16 nodes with the accelerometer attached at 6th node

6.4 Application on fixed-beam

An experimental setup of a steel beam fixed at both ends is considered to observe the effect of the weight of the attached accelerometer (Fig. 21). The weight of the beam is kept much higher than that of the accelerometer. The fixity at the ends is provided by bolts and welding over the projected flange of a clip angle connected over a large-angle section. The steel beam has a cross-section of $7.5 \text{ cm} \times 10 \text{ cm}$ and a modulus of elasticity of 200 GPa. The cross-section of the projected angle is measured as $10 \text{ cm} \times 1 \text{ cm}$. The total clear span length of the beam left after connection with the projected angle is 55 cm. It is observed during initial trials that the effective length of beam contributing towards vibration also includes the length of the projected flanges also, observable from Fig. 21. Hence, the total end-to-end distance of 75 cm is considered for optimization. The test structure is divided into 15 equal elements consists of 16 nodes for hammering. The accelerometer is attached at the 6th node, as shown in Fig. 21.

The roving impact hammer test is repeated at all the 16 nodes, and response is collected at the 6th node. In this case, a hard hammer tip is used because of the high stiffness of the structure. The first six experimental frequencies and the mode shapes extracted are shown in Fig. 22. It is noted that due to some noise and experimental uncertainty while hammering, the second mode shape is showing unusual curvature. The numerical model is updated with the obtained experimental responses. The parameters used for optimization are 1 cm, 0.6 cm, 3.5 cm, and 30000 as the initial value, the upper bound, the lower bound, and the function evaluations limit, respectively. The upper bound of depth is kept high to incorporate the large depth due to the presence of flange, bolts, and welded connection. The optimized depth results are shown in Fig. 23.

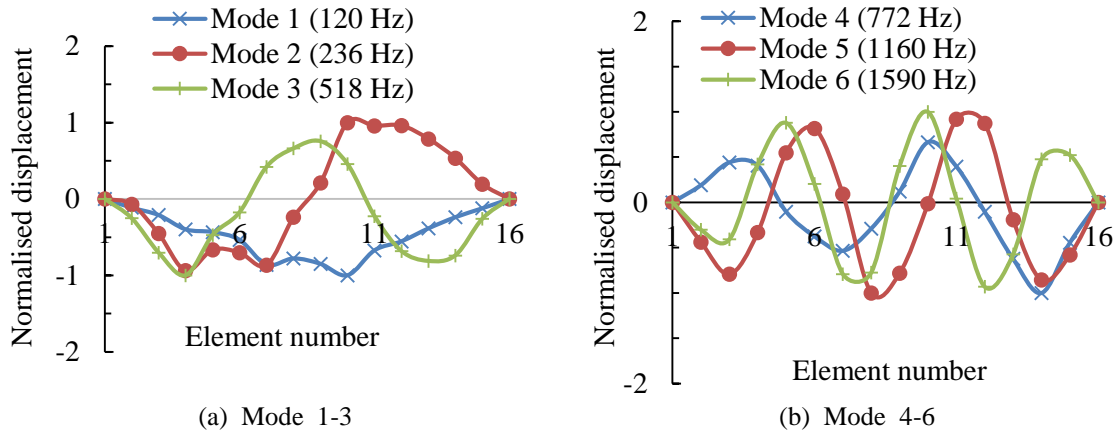


Fig. 22 Experimental mode shapes of the considered fixed beam

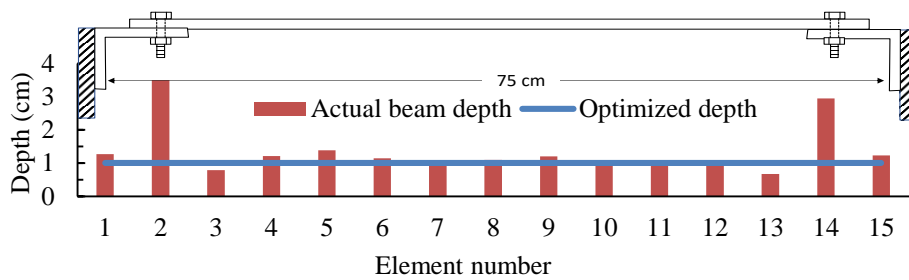


Fig. 23 Optimized depth results of the considered fixed beam after model updating

The optimized result shows that the end element on each of the side has slightly lesser depth, which is expected just after the end of the beam, i.e., the depth of flange only. The 2nd and 14th elements are showing large depth replicating higher stiffness in that location, which is due to the effect of connection of projected flange and beam and presence of large size bolt in that element. There is a sudden stiffness decrease shown in the 3rd and 13th elements, which is due to the end of the projected flanges connected with the beam. All other elements show almost equal depth with a small number of variations due to noises and errors in the extraction of experimental responses. It is observed that even with visible noise in the second mode, the method is able to identify the variation of stiffness over the structure, with reasonable accuracy in identifying damages. Also, it can be seen that there is some level of false detections, but the approach is efficient in identifying sudden changes of depth, thus the stiffness.

7. Conclusions

This study presents a SHM approach for old and existing structures. The damages are detected by numerical model updating technique via optimization using the initial designed structural properties as its undamaged state. The method uses structural engineering code OpenSees for

numerical modelling and NOMAD optimization code for model updating. The use of OpenSees makes the FE modelling of complex structures much simpler. Also, both the codes being open-sourced makes the proposed approach economical. Modal analysis is used for damage identification. The studies presented here include the choice of effective modes, an adequate objective function, and a comparison between available frequency and mode shape-based objective functions. The effectiveness of NOMAD optimization is compared with ALO and TLBO algorithms. A cantilever beam is used with single and multiple damage cases to check the efficacy of the proposed method. Moreover, a more realistic damage scenario of decreased as well as increased stiffness are also considered in a fixed beam. Numerical and experimental validations via impact hammer test are performed and the following significant conclusions have been drawn:

- (i) Natural frequency alone can be used for broad and rough damage detection; however, if both the mode shapes along with the natural frequencies are incorporated in the objective function (OF^*), it will add the local state of the structure and will enhance the optimization results. The objective function OF^* took lesser time for optimization and the least average error (14%) in each element than similar objective functions available in the literature.
- (ii) At least five modal responses are needed for optimization and damage detection with acceptable error and computational time.
- (iii) The approach proposed here was effective in identifying the locations of damage along with the intensities for all the numerical damage scenarios considered.
- (iv) The method also proved efficient in the identification of damage locations as well as the intensity of the damaged beam experimentally tested. The depth identification is with less than 2% error at damage location and 14% error globally.
- (v) In the tests on the fixed beam, the method can identify the increased stiffness at bolt locations via showing increased depth values. This case is the replica of the concept of stiffness variation over the structure presented here. Also, this is the best example of increased stiffness over a particular zone, and the method can locate the same.
- (vi) From the comparative study, it is observed that NOMAD takes lesser evaluations of the objective function and the ultimate results of optimization are consistent with the presently available optimization algorithms.

Overall, the presented damage detection method is simple, economical, and user-friendly in numerical modelling and use. And can be used for the global identification of stiffness irregularity which will replicate the probable damage. It performed well in assessing damage location and damage severity for the studied problems, and further studies are needed for its applicability over real-time complex civil engineering structures. Efficiency of the method in getting minor damage has been examined numerically, and the same can be done experimentally with a wide range of damage levels in future. Furthermore, more studies are required to deal with the issue of inappropriate or incomplete measurements.

Funding

This work is supported by the Ministry of Human Resource Development, Government of India.

References

Arefi S.L. and Gholizad A. (2020), "Damage identification of structures by reduction of dynamic matrices

- using the modified modal strain energy method”, *Struct. Monit. Maint.*, **7**(2), 125-147. <https://doi.org/10.12989/smm.2020.7.2.125>.
- Audet, C. and Dennis Jr, J.E. (2006), “Mesh adaptive direct search algorithms for constrained optimization”, *Soc. Ind. Appl. Math.*, **17**(1), 188-217. <https://doi.org/10.1137/040603371>.
- Audet, C. and Hare, W. (2017), *Derivative-Free and Blackbox Optimization*, Springer Series in Operations Research and Financial Engineering, Springer International Publishing, Switzerland. <https://doi.org/10.1007/978-3-319-68913-5>.
- Azim, M.R., Zhang, H. and Mustafa, G. (2020), “Damage detection of railway bridges using operational vibration data: theory and experimental verifications”, *Struct. Monit. Maint.*, **7**(2), 149-166. <https://doi.org/10.12989/smm.2020.7.2.149>.
- Bahrami, S., Tribes, C., Devals, C., Vu, T.C. and Guibault, F. (2016), “Multi-fidelity shape optimization of hydraulic turbine runner blades using a multi-objective mesh adaptive direct search algorithm”, *Appl. Math. Model.*, **40**, 1650-1668. <https://doi.org/10.1016/j.apm.2015.09.008>.
- Barman, S.K., Maiti, D.K. and Maity, D. (2020), “Damage detection of truss employing swarm-based optimization techniques: A comparison”, *Advanced Engineering Optimization Through Intelligent Techniques*, **949**, 21-37. https://doi.org/10.1007/978-981-13-8196-6_3.
- Beck (2010), “Bayesian system identification based on probability logic”, *Struct. Control Health Monitoring*, **17**, 825-847. <https://doi.org/10.1002/stc.424>.
- Behmanesh, I. and Moaveni, B. (2015), “Probabilistic identification of simulated damage on the Dowling Hall footbridge through Bayesian finite element model updating”, *Struct. Control Health Monit.*, **22**(3), 463-483. <https://doi.org/10.1002/stc.1684>.
- Behmanesh, I., Moaveni, B., Lombaert, G. and Papadimitriou, C. (2015), “Hierarchical Bayesian model updating for structural identification”, *Mech. Syst. Signal Pr.*, **64**, 360-376. <https://doi.org/10.1016/j.ymsp.2015.03.026>.
- Ching, J., Beck, J.L. and Porter, K.A. (2006), “Bayesian state and parameter estimation of uncertain dynamical systems”, *Probabilist. Eng. Mech.*, **21**(1), 81-96. <https://doi.org/10.1016/j.probengmech.2005.08.003>.
- Dinh-cong, D., Nguyen-thoi, T. and Nguyen, D.T. (2020), “A FE model updating technique based on SAP2000-OAPI and enhanced SOS algorithm for damage assessment of full-scale structures”, *Appl. Soft Comput. J.*, **89**, 106100. <https://doi.org/10.1016/j.asoc.2020.106100>.
- Dubé, O., Dubé, D., Chaouki, J. and Bertrand, F. (2014), “Optimization of detector positioning in the radioactive particle tracking technique”, *Appl. Radiation Isotopes*, **89**, 109-124. <https://doi.org/10.1016/j.apradiso.2014.02.019>.
- Erazo, K., Moaveni, B. and Nagarajaiah, S. (2019), “Bayesian seismic strong-motion response and damage estimation with application to a full-scale seven story shear wall structure”, *Eng. Struct.*, **186**, 146-160. <https://doi.org/10.1016/j.engstruct.2019.02.017>.
- Erazo, K. and Nagarajaiah, S. (2017), “An offline approach for output-only Bayesian identification of stochastic nonlinear systems using unscented Kalman filtering”, *J. Sound Vib.*, **397**, 222-240. <https://doi.org/10.1016/j.jsv.2017.03.001>.
- Farrar, C., Doebling, S. and Nix, D. (2001), “Vibration-based structural damage identification”, *Philos. T. R. Soc. A*, **359**, 131-149. <https://doi.org/10.1098/rsta.2000.0717>.
- Fowler, K.R., Reese, J.P., Kees, C.E., Dennis Jr, J.E., Kelley, C.T., Miller, C.T., Audet, C., Booker, A.J., Couture, G., Darwin, R.W., Farthing, M.W., Finkel, D.E., Gablonsky, J.M., Gray, G., and Kolda, T.G. (2008), “Comparison of derivative-free optimization methods for groundwater supply and hydraulic capture community problems”, *Adv. Water Resour.*, **31**(5), 743-757. <https://doi.org/10.1016/j.advwatres.2008.01.010>.
- Inman, D., Farrar, C. and Lopes, V. (2005), *Damage Prognosis: For Aerospace, Civil and Mechanical Systems*, Wiley.
- Jafarkhani, R. and Masri, S.F. (2011), “Finite Element Model Updating Using Evolutionary Strategy for Damage Detection”, *Comput. - Aided Civil Infrastruct. Eng.*, **26**(3), 207-224. <https://doi.org/10.1111/j.1467-8667.2010.00687.x>.

- Jaiswal, D.K., Dash, S.R. and Mondal, G. (2020), "Development of an effective and efficient baseline free damage detection scheme for structural health monitoring", *Proceedings of the Indian Structural Steel Conference*, Hyderabad, India, March.
- Jin, S. and Jung, H. (2016), "Sequential surrogate modeling for efficient finite element model updating", *Comput. Struct. J.*, **168**, 30-45. <https://doi.org/10.1016/j.compstruc.2016.02.005>.
- Jin, S.S., Cho, S., Jung, H.J., Lee, J.J. and Yun, C.B. (2014), "A new multi-objective approach to finite element model updating", *J. Sound Vib.*, **333**(11), 2323-2338. <https://doi.org/10.1016/j.jsv.2014.01.015>.
- Kaveh, A. and Zolghadr, A. (2017), "Guided modal strain energy-based approach for structural damage identification using tug-of-war optimization algorithm", *J. Comput. Civil Eng.*, **31**(4), 04017016. [https://doi.org/10.1061/\(ASCE\)CP.1943-5487.0000665](https://doi.org/10.1061/(ASCE)CP.1943-5487.0000665).
- Khatir, S., Dekemele, K., Loccufer, M., Khatir, T. and Wahab, M.A. (2018), "Crack identification method in beam-like structures using changes in experimentally measured frequencies and Particle Swarm Optimization", *Comptes Rendus Mécanique*, **346**(2), 110-120. <https://doi.org/10.1016/j.crme.2017.11.008>.
- Khatir, S., Wahab, M.A., Boutchicha, D. and Khatir, T., (2019), "Structural health monitoring using modal strain energy damage indicator coupled with teaching-learning-based optimization algorithm and isogeometric analysis", *J. Sound Vib.*, **448**, 230-246. <https://doi.org/10.1016/j.jsv.2019.02.017>.
- Le Digabel, S. (2011), "Algorithm 909: NOMAD: Nonlinear optimization with the MADS algorithm", *ACM T. Math. Software*, **37**(4), 1-15. <https://doi.org/10.1145/1916461.1916468>.
- Majumdar, A., Nanda, B., Maiti, D.K. and Maity, D. (2014), "Structural damage detection based on modal parameters using continuous ant colony optimization", *Adv. Civil Eng.*, **2014**, 1-14. <https://doi.org/10.1155/2014/174185>.
- McKenna, F. (2011), "OpenSees: a framework for earthquake engineering simulation", *Comput. Sci. Eng.*, **13**(4), 58-66. <https://doi.org/10.1109/MCSE.2011.66>.
- Meruane, V. and Heylen, W. (2011), "An hybrid real genetic algorithm to detect structural damage using modal properties", *Mech. Syst. Signal Pr.*, **25**(5), 1559-1573. <https://doi.org/10.1016/j.ymsp.2010.11.020>.
- Mirjalili, S. (2015), "The ant lion optimiser", *Adv. Eng. Softw.*, **83**, 80-98. <https://doi.org/10.1016/j.advengsoft.2015.01.010>.
- Mishra, M., Barman, S.K., Maity, D. and Maiti, D.K. (2019), "Ant lion optimization algorithm for structural damage detection using vibration data", *J. Civil Struct. Health Monit.*, **9**(1), 117-136. <https://doi.org/10.1007/s13349-018-0318-z>.
- Mishra, M., Barman, S.K., Maity, D. and Maiti, D.K. (2020), "Performance studies of 10 metaheuristic techniques in determination of damages for large-scale spatial trusses from changes in vibration responses", *J. Comput. Civil Eng.*, **34**(2), 04019052. [https://doi.org/10.1061/\(ASCE\)CP.1943-5487.0000872](https://doi.org/10.1061/(ASCE)CP.1943-5487.0000872).
- Moaveni, B., He, X., Conte, J.P. and De Callafon, R.A. (2008), "Damage identification of a composite beam using finite element model updating", *Comput. - Aided Civil Infrastruct. Eng.*, **23**(5), 339-359. <https://doi.org/10.1111/j.1467-8667.2008.00542.x>.
- Moaveni, B., He, X., Conte, J.P. and Restrepo, J.I. (2010), "Damage identification study of a seven-story full-scale building slice tested on the UCSD-NEES shake table", *Struct. Saf.*, **32**(5), 347-356. <https://doi.org/10.1016/j.strusafe.2010.03.006>.
- Moaveni, B., Hurlbaas, S. and Moon, F. (2013), "Special issue on real-world applications of structural identification and health monitoring methodologies", *J. Struct. Eng. - ASCE*, **139**(10), 1637-1638. [https://doi.org/10.1061/\(ASCE\)ST.1943-541X.0000779](https://doi.org/10.1061/(ASCE)ST.1943-541X.0000779).
- Mohan, S.C., Maiti, D.K. and Maity, D. (2013), "Structural damage assessment using FRF employing particle swarm optimization", *Appl. Math. Comput.*, **219**(20), 10387-10400. <https://doi.org/10.1016/j.amc.2013.04.016>.
- Nagarajaiah, S. and Erazo, K. (2016), "Structural monitoring and identification of civil infrastructure in the United States", *Struct. Monit. Maint.*, **3**(1), 51-69. <http://dx.doi.org/10.12989/smm.2016.3.1.051>.
- Nguyen, C., Huynh, T.C. and Kim, T. (2018), "Vibration-based damage detection in wind turbine towers using artificial neural networks", *Struct. Monit. Maint.*, **5**(4), 507-519. <https://doi.org/10.12989/smm.2018.5.4.507>.

- Pastor, M., Binda, M. and Harčarik, T. (2012), "Modal assurance criterion", *Procedia Eng.*, **48**, 543-548. <https://doi.org/10.1016/j.proeng.2012.09.551>.
- Qiao, P. and Fan, W. (2014), "Lamb wave-based damage imaging method for damage detection of rectangular composite plates", *Struct. Monit. Maint.*, **1**(4), 411-425. <http://dx.doi.org/10.12989/smm.2014.1.4.411>.
- Rao, R.V., Savsani, V.J. and Vakharia, D.P. (2011), "Teaching-learning-based optimization: A novel method for constrained mechanical design optimization problems", *Comput. Aided Design*, **43**(3), 303-315. <https://doi.org/10.1016/j.cad.2010.12.015>.
- Rao, R.V., Savsani, V.J. and Vakharia, D.P. (2012), "Teaching-learning based optimization: An optimization method for continuous nonlinear large scale problems", *Inform. Sci.*, **183** (1), 1-15. <https://doi.org/10.1016/j.ins.2011.08.006>.
- Razavi, M. and Hadidi, A. (2020), "Assessment of sensitivity-based FE model updating technique for damage detection in large space structures", *Struct. Monit. Maint.*, **7**(3), 261-281. <https://doi.org/10.12989/smm.2020.7.3.261>.
- Rios, L. And Sahinidis, N. (2010), "Derivative-free optimization: A review of algorithms and comparison of software implementations", *J. Global Optim.*, **56**(3), 1247-1293. <https://doi.org/10.1007/s10898-012-9951-y>.
- Schallhorn, C. and Rahmatalla, S. (2015), "Crack detection and health monitoring of highway steel-girder bridges", *Struct. Health Monit.*, **14**(3), 281-299. <https://doi.org/10.1177/1475921714568404>.
- Smyl, D., Pour-Ghaz, M. and Seppänen, A. (2018), "Detection and reconstruction of complex structural cracking patterns with electrical imaging", *NDT & E Int.*, **99**, 123-133. <https://doi.org/10.1016/j.ndteint.2018.06.004>.
- Som, S., Maity, S., Som, B. and Sur, S. (2019), *Dominant Failure Path Prediction Of Majherhat Bridge Collapse At Kolkata*, Indian Highways, June, **47**(6), 20-29.
- Stubbs, N. and Kim, J.T. (1996), "Damage localization in structures without baseline modal parameters", *AIAA J.*, **34**(8), 1644-1649. <https://doi.org/10.2514/3.13284>.
- Sun, H., and Buyukozturk, O. (2016), "Bayesian model updating using incomplete modal data without mode matching", *Proceedings of SPIE*, **9805**, 108-116. <https://doi.org/10.1117/12.2219300>.
- Varma, T.V., Sarkar, S. and Mondal, G. (2020), "Buckling restrained sizing and shape optimization of truss structures", *J. Struct. Eng.*, **146**(5), 04020048. [https://doi.org/10.1061/\(ASCE\)ST.1943-541X.0002590](https://doi.org/10.1061/(ASCE)ST.1943-541X.0002590).
- Wu, M. and Smyth, A.W. (2007), "Application of the unscented Kalman filter for real-time nonlinear structural system identification", *Struct. Control Health Monit.*, **14**(7), 971-990. <https://doi.org/10.1002/stc.186>.
- Zanardo, G., Hao, H., Xia, Y. and Deeks, A.J. (2006), "Stiffness assessment through modal analysis of an RC slab bridge before and after strengthening", *J. Bridge Eng.*, **11**(5), 590-601. [https://doi.org/10.1061/\(ASCE\)1084-0702\(2006\)11:5\(590\)](https://doi.org/10.1061/(ASCE)1084-0702(2006)11:5(590)).